Zeitschrift: Swiss bulletin für angewandte Geologie = Swiss bulletin pour la géologie appliquée = Swiss bulletin per la geologia applicata = Swiss bulletin for applied geology

Herausgeber: Schweizerische Vereinigung von Energie-Geowissenschaftern; Schweizerische Fachgruppe für Ingenieurgeologie

Band: 25 (2020)

Heft: 1-2

Artikel: Monitoring slow-moving landslides in Switzerland with satellite SAR interferometry

Autor: Strozzi, Tazio / Caduff, Rafael / Manconi, Andrea

DOI: https://doi.org/10.5169/seals-977310

Swiss Bull. angew. Geol. Vol. 25/1+2, 2020 S. 85-99

Monitoring slow-moving landslides in Switzerland with satellite SAR interferometry

Tazio Strozzi[1], Rafael Caduff[1], Andrea Manconi[1], Urs Wegmüller[1] and Christian Ambrosi[2]

Keywords
Canton Ticino, satellite SAR interferometry, landslide, surface displacement.

Abstract
Accurate information about the surface deformation of slope instabilites is important for the analysis and interpretation of their associated hazard potential. Satellite SAR interferometry is an appealing technology for surface deformation monitoring over large areas that is now entering an advanced operational phase triggered by the increased availability of satellite data. In order to show potential and limitations of current satellite SAR data for the assessment of the state of activity of slow-moving landslides in Switzerland, we exemplary present results over Loderio in Canton Ticino. By the synergetic use of satellite SAR data of different carrier frequencies and ground resolutions, we could detect both the fastest moving and vegetated part of the landslide (rates of motion up to 6 cm/year) as well as rocks and scattered houses over the very slow-moving sectors (rates of motion of a few mm/year up to 1 cm/year). The satellite based information on the surface motion complements well the geomorphological analysis performed with aerial photographs and field surveys. Similar results can be nowadays expected everywhere over slow-moving landslides in the Swiss Alps.

1 Introduction

Over Switzerland, hazards due to slope instabilities affect about 6% of the territory (Lateltin et al., 2005). In many cases, slope instabilities produce surface displacement, which is an important parameter to interpret their current state of activity as well as to identify potential changes in their spatial and temporal behaviour. It is therefore extremely important to continuously monitor the rate of motion of landslides for the assessment of their hazard potential (Raetzo and Loup, 2016). In particular, there is a gap in knowledge on spatial and temporal characteristics of slow-moving landslides, which can slip slowly for decades and then suddenly accelerate and potentially lead to fatal effects (Palmer, 2017; Krähenbühl and Nänni, 2017). Satellite Synthetic Aperture Radar (SAR) interferometry (InSAR) is one option for surface deformation monitoring over large areas (Bamler and Hartl, 1998; Rosen et al., 2000). This technology is now entering an andvanced operational phase, triggered by the increased availability of satellite data and in particular by regular acquisitions provided by Sentinel-1 data since 2014. This led to an emerging trend, i.e. country-scale maps of land deformation recently released

[1] Gamma Remote Sensing, Worbstrasse 225, 3073 Gümligen, Switzerland
{strozzi;caduff;manconi;wegmuller}@gamma-rs.ch
[2] Institute of Earth Sciences, University of Applied Sciences and Arts of Southern Switzerland (SUPSI), Campus Trevano, CH-6952 Canobbio, Switzerland
christian.ambrosi@supsi.ch

in Norway[1] and Germany[2] . Products of this kind are of high interest also in Switzerland, where regularly updated deformation maps from InSAR would be beneficial for operational monitoring of slope instabilities, as well as for other natural processes or infrastructures.

In this contribution we examine how satellite SAR interferometry can be efficiently employed in Switzerland to characterize the status of activity of slow-moving landslides, i.e. landslides with rates of motion of a few cm/year according to Cruden and Varnes (1996). As an example of such a large and active, despite very slow landslide we consider the Loderio landslide in Canton Ticino. We discuss the potential and the limitations of current satellite SAR data with different carrier frequencies (L-, C- and X-band), ground resolutions (around 10, 20 and 2 meters), time intervals (46, 6, 24 and 11 days) and acquisition strategies (global versus on-demand, free versus commercial data) and we highlight advantages and disadvantages of results obtained using various multi-temporal interferometric approaches based on large data stacks (e.g. Ferretti et al., 2001; Berardino et al., 2002; Wegmüller et al., 2003; Hooper, 2008). We wrap up by illustrating what is the added value of satellite SAR interferometry compared to the classic geomorphological approach.

2 Satellite SAR missions

In this section we give a short overview of the main historical and current satellite SAR missions (Table 1). We focus our attention on sensors with a comparatively open distribution strategy from national or international space agencies. Other current or upcoming national (e.g. RISAT from the Indian Space Research Organisation or SAOCOM from the Argentina's space agency) or commercial (e.g the constellations of SAR satellites from the Finnish manufacturer ICEYE or the US company Capella Space) missions, with a more restricted data access, are not considered in this review.

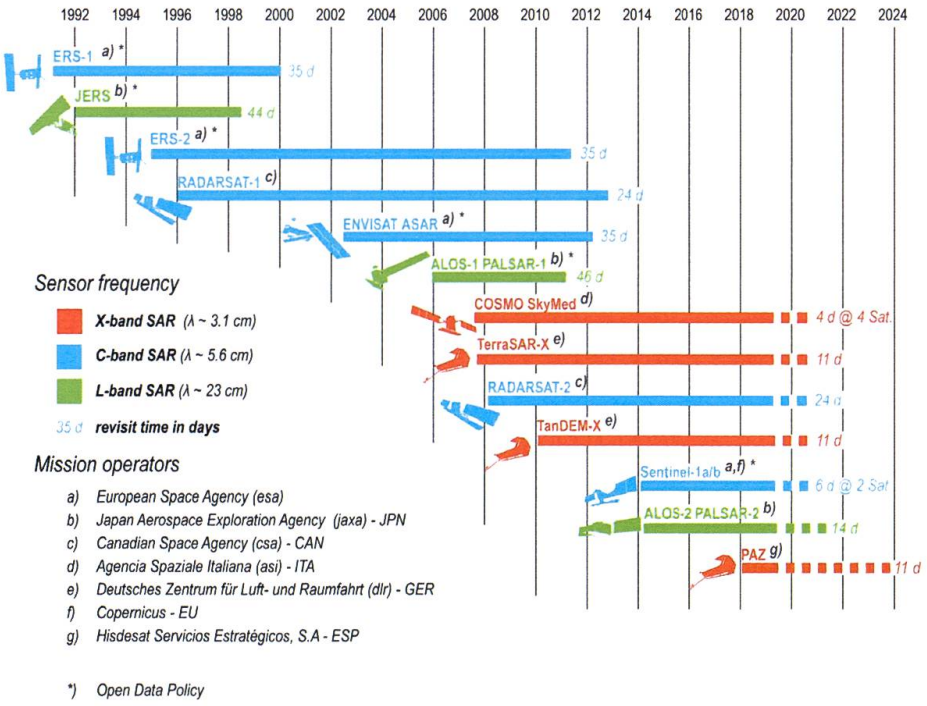

Table 1: Overview of the main historical and current satellite SAR missions.

[1] https://insar.ngu.no
[2] https://bodenbewegungsdienst.bgr.de

The very first mission that operated for 106 days a SAR sensor from space at L-band (1.3 GHz, 23.5 cm wavelength) was the NASA mission SEASAT in 1978. SAR data at L-band were then operationally acquired by the Japan Aerospace Exploration Agency JAXA with the JERS-1 (1992-1998), ALOS-1 PALSAR-1 (2006-2011) and ALOS-2 PALSAR-2 (2014-ongoing) missions. In order to optimize the downlink capacity, the L-band Japanese missions follow a systematic acquisition strategy, with only a few images acquired globally every year, despite the fact that the nominal repeat cycles of the satellites were between 14 and 46 days. While the historical SAR images from JERS-1 and ALOS-1 PALSAR-1 are now distributed following a free and open data policy, those from ALOS-2 PALSAR-2 are available commercially or in the framework of research projects for a limited (e.g. < 100) number of images.

The European Space Agency (ESA) has been providing repeated SAR data at C-band (5.3 GHz, 5.7 cm wavelength) since the beginning of the 1990's with the ERS-1 (1991-2000), ERS-2 (1995-2011) and ENVISAT (2002-2010) missions. The Sentinel-1 constellation – ESA follow-on SAR mission specifically designed for SAR interferometric applications and displacement monitoring – is operational since 2014 and has an expected lifetime of 20 years. With both Sentinel 1A and Sentinel-1B satellites in operation since 2016, SAR images from the same orbit are acquired every 6 days over Europe and distributed shortly after acquisition following a free and open data policy. Also Canada has been operating a series of SAR missions at C-band, Radarsat-1 (1996-2013), Radarsat-2 (2007-ongoing) and the RADARSAT Constellation Mission, launched in 2019 to provide continuous C-band SAR data from a fleet of three satellites. These Canadian missions are tailored to applications in Canada or following a commercial strategy. In Switzerland, Radarsat-2 data from the snow-free period from May to October of every year were regularly programmed since 2011 over the Alps by the Federal Office for the Environment.

The Cosmo-SkyMed constellation of four satellites, launched in 2007, and the three identical sensors TerraSAR-X, TanDEM-X and PAZ, launched in 2007, 2010 and 2018, respectively, operate at X-band (9.65 GHz, 3.1 cm wavelength). The higher frequency allows to work with a larger bandwidth and thus to achieve a higher range resolution. These missions are based on public / commercial / military agreements within Italy, Germany and Spain and data are mainly available on-demand. In Switzerland, TerraSAR-X data from the snow-free period from May to October of every year were regularly programmed since 2011 over parts of the Alps by the Federal Office for the Environment, while for some other regions data are available in the framework of research projects. Cosmo-Skymed images were only regularly acquired at the border to Italy, where a nation-wide acquisition programme (MAP Italy) is in place for the mapping of the entire country every 16 days. Cosmo-Skymed images are available commercially or in the framework of research projects for a limited number of images.

3 Satellite SAR interferometry

In this section, we recall the state-of-the-art SAR interferometric algorithms for deformation monitoring. We first introduce the basic principle of SAR interferometry (InSAR) for single image pairs. Then, processing strategies for large stacks of SAR images, including commonly used algorithms such as Persistent Scatterer Interferometry (PSI) and Multi-looked Temporal Interferometry (MTI), are described. In this context, we highlight peculiarities of InSAR processing over the Alps, where sparse urbanization, large vegetated areas, snow-cover, layover/shadow, and atmospheric stratification and summer turbulences, introduce specific challenges.

InSAR is a method whereby two SAR satellite acquisitions of different times covering largely the same area with a slight orbital offset are combined and their phase difference is measured (Bamler and Hartl, 1998; Rosen et al., 2000). This phase offset relates to both the topographic height and movement in the satellite line-of-sight (LOS). Differential InSAR (DinSAR) removes the topographic phase of the acquired signals and enables detection of surface movement at variable time scales depending on the selected time-interval, effectively creating, after phase unwrapping (i.e. adding the appropriate multiples of 2π to the phase delay), an absolute displacement map in the LOS. DInSAR is a popular and widely used application in mountain areas, as it allows systematic and continuous monitoring of entire landforms at a scale ranging from simple slope faces to whole mountain ranges at high spatial resolution (Colesanti and Wasowski, 2006; Delacourt et al., 2007; Herrera et al., 2009; Strozzi et al., 2010). However, it is typically affected by several errors which need to be corrected for, such as atmospheric effects, geometric influences, and signal noise. Atmospheric turbulence and stratification can range several cm's of apparent motion and induce errors in phase unwrapping. Layover and shadowing are common effects in rugged terrain, which reduce the spatial coverage. Vegetation is increaseing the phase noise (i.e. decreasing the image coherence, a value which ranges from 0 (just noise) to 1 (complete absence of phase noise)), in particular for long time-interval. Images acquired during late autumn, winter and early spring months, often dominated by low coherence over snow cover and subsequent snow melt, limit the temporal coverage of InSAR in mountainous regions, while late spring to early autumn months allow regular coverage of good coherence (Wasowski and Bovenga, 2014).

In PSI, DInSAR is applied on selected pixels that exhibit a point-target scattering behaviour and are persistent over an extended observation time period (Ferretti et al., 1999; Wegmüller et al., 2013). Through the use of many SAR scenes, errors resulting from atmospheric inhomogeneities are reduced and a higher accuracy can be achieved. Over built-up areas, with numerous man-made structures, or in regions where exposed rocks or single infrastructures are visible, it is possible to estimate the progressive deformation of the terrain at millimetre accuracy. In mountainous regions, the number of persistent scatterers is however limited by the sparse urbanization, the large forest cover, and areas of shadow and layover (Strozzi et al., 2013; Wegmüller et al., 2013). In addition, also for PSI snow-cover causes low coherence during winter months. If only snow-free acquisitions from late spring to early autumn of every year are considered, gaps in the interferogram time-series limit the intervals over which reliable phase unwrapping can be performed. As a consequence, only rates of motion of less than a few cm's per year can be determined.

PSI requires large data stacks to reliably identify the point targets, unwrap the phase, and mitigate the atmospheric disturbances. MTI, combining a number of multi-looked unwrapped interferograms to increase the signal to noise ratio and mitigate the atmospheric disturbances, offers an alternative to work with a reduced number of images, as in our case study for ALOS-2 PALSAR-2 data. A set of interferograms can be combined via stacking or inverted in some way to solve for the temporal displacement (Berardino et al., 2002; Schmidt and Bürgmann, 2003, Werner et al., 2012). Multi-looked interferograms also give the opportunity to consider other targets known as distributed scatterers (DS), which are associated with ground resolution cells occurring mainly in rural areas, such as agricultural terrain or pastures (Samiei-Esfahany et al., 2016). PSI and MTI methods can be also combined to extract signal from more pixels than either method can achieve alone (Hooper, 2008).

The accuracy of InSAR and PSI/MTI results in the LOS direction was estimated in various experiments in the past. While the limit of accuracy of PSI with C-band data is between 1.0 to 1.8 mm/year over a time period of 5 years for the average displacement rate and between 4.2 and 6.1 mm for single deformation measurements (Crosetto et al., 2009), that of MTI with ALOS-1/2 PALSAR-1/2 over a time period of 4 years is on the order of 9 mm/year for the deformation rate (Ng et al., 2012) and of 14 to 15 mm for single measurements (Sandwell et al., 2008; Nishiguchi et al. (2017).

4 Loderio landslide

In order to discuss potential and limitations of current satellite SAR data for the monitoring of very slow landslides in Switzerland, we analysed the Loderio landslide in Canton Ticino (Figures 1 and 2). The Loderio mass movement occupies the right-hand side of the Blenio valley just north of the village Biasca, extending from the bottom of the valley at about 350 m a.s.l. to more than 2,000 m a.s.l. This movement is an example of a deep-seated gravitational slope deformation (DGSD, e.g., Dramis and Sorriso-Valvo, 1994; Noverraz et al., 1998) in crystalline rocks of the Central Alps and it covers an area of about 9.5 km^2. In Ticino, the climate is temperate and within a certain variability characterized by normally dry and sunny winters, with periods of föhn from the north but also with sometimes abundant snowfalls, from precipitations above all in the seasons of transition (spring and autumn), and from sunny summers often interrupted by violent showers. This allows the growth of a forest of many species, including in our area of interest chestnuts and birches at lower altitudes turning to beech trees and spruces at higher altitudes (Fig. 1). Above the settlements at the bottom of the valley only scattered holiday houses are present within the forest and meadows, with accumulation of debris visible in particular at the southern section of the landslide.

The ridge of the Loderio landslide is composed of the Ordovician gneiss with foliation dipping towards the valley. This huge slope deformation can be divided into three sectors, that are showing different morphological and kinematic characteristics (Fig. 2). The northern sector, on east of (i.e. above) Semione, does not appear to be particularly active. The upper part of the slope, above the 1,500 m a.s.l., is characterized by a series of scarps and associated counter scarps directed NW-SW that looks eroded and partially covered by a glacial deposit. In the medium-lower part the slope is affected by a series of scarps directed N-S associated with diffuse rockfalls and debris accumulations. In its central sector around Bü the Loderio DGSD is characterized by the presence, at about 1,500 m a.s.l., of a huge scarp trending NE-SW. At the east of this scarp the rock mass appears to be strongly fractured and locally disintegrated by the presence of a series of rockslides. A series of active scarps and tension cracks suggest the presence of an active rockslide suspended above 1,250 m.

The southern sector of the Loderio DGSD is affected by a series of active rockslides that cover an area of about 2 km^2. In this area numerous scarps and open tension cracks directed NW-SE develop in the upper part of the rock scarp of about 60 m high and 1,300 m long located NE of Loderio between 800 and 1,300 m a.s.l. These open tension cracks cause slides and tilt of the rock mass that is consequently affected by frequent rockfalls. The main part of the collapsed rock mass - called Ganne di Mornatt - had stopped at the toe of the scarp. In the most southern part of the slope an active complex rockslide is present. The rockslide accumulation, collapsed from a NE-SW scarp at 800 m a.s.l. with an estimated volume of about 3.5 Mm^3, reached the toe of the slope causing an im-

Fig. 1: Photograph of the Loderio landslide (courtesy F. Strozzi) and of trenches in the upper part of the slope (courtesy S. Daverio).

portant deviation and probably a temporary dam of the main river. Structural and geological mapping of the area indicates that the geology associated to the foliation of the gneiss play an important role in the development of this complex rockslide. The scarp of the rockslide is located at the contact between ultramaphite and gneiss and controlled by the pre-existing dep slope foliation planes. Indeed, in this part of the slope fractured gneiss covers with low thickness the below hardly ultramaphite.

5 Results

In this work over the Loderio landslide we considered the following four image stacks:

- 17 ALOS-2 PALSAR-2 images acquired between 2014.09.06 and 2018.10.13 with a nominal repeat cycle of 42 days and a ground resolution of about 10 m;
- 42 Radarsat-2 images acquired between 2011.05.05 and 2017.10.12 with a nominal repeat cycle of 24 days and a ground

resolution of about 20 m until 2015 and of about 5 m since 2016:

- 88 Sentinel-1 images acquired between 2015.05.10 and 2018.10.15 with a nominal repeat cycle of 12 days until 2016 and of 6 days since 2017 and a ground resolution of about 20 m;
- 50 TerraSAR-X images acquired between 2014.05.21 and 2017.10.26 with a nominal repeat cycle of 11 days and a ground resolution of about 3 m.

For our analyses we mainly used images acquired under snow-free conditions and disregarded therefore data from November to April of every year. Due to the limited availability of imagery, only for ALOS-2 PALSAR-2 five winter images were retained in order to increase the data available for multi-temporal interferometry.

Differential interferograms computed at the end of the summer / beginning of autumn over one satellite cycle from TerraSAR-X, Sentinel-1 and Radarsat-2 and over 56 days (4 satellite cycles) from ALOS-2 PALSAR-2 are presented in Figure 3. In such a short time period, the displacement of the landslide cannot be recognised and the large-scale phase shifts are due to atmospheric artefacts. We use these images in order to discuss how the phase noise varies for the different DInSAR data considered in our study. ALOS-2 PALSAR-2 shows a fairly good coherence (or low phase noise) in particular over the bottom of the valley and the meadows at higher elevations, but the phase signal is also visible over forested areas. To the north, the coverage of some of the ALOS-2 PALSAR-2 data we could consider for our analyses is not complete. With TerraSAR-X a fairly good coherence can be again observed at the bottom of the val-

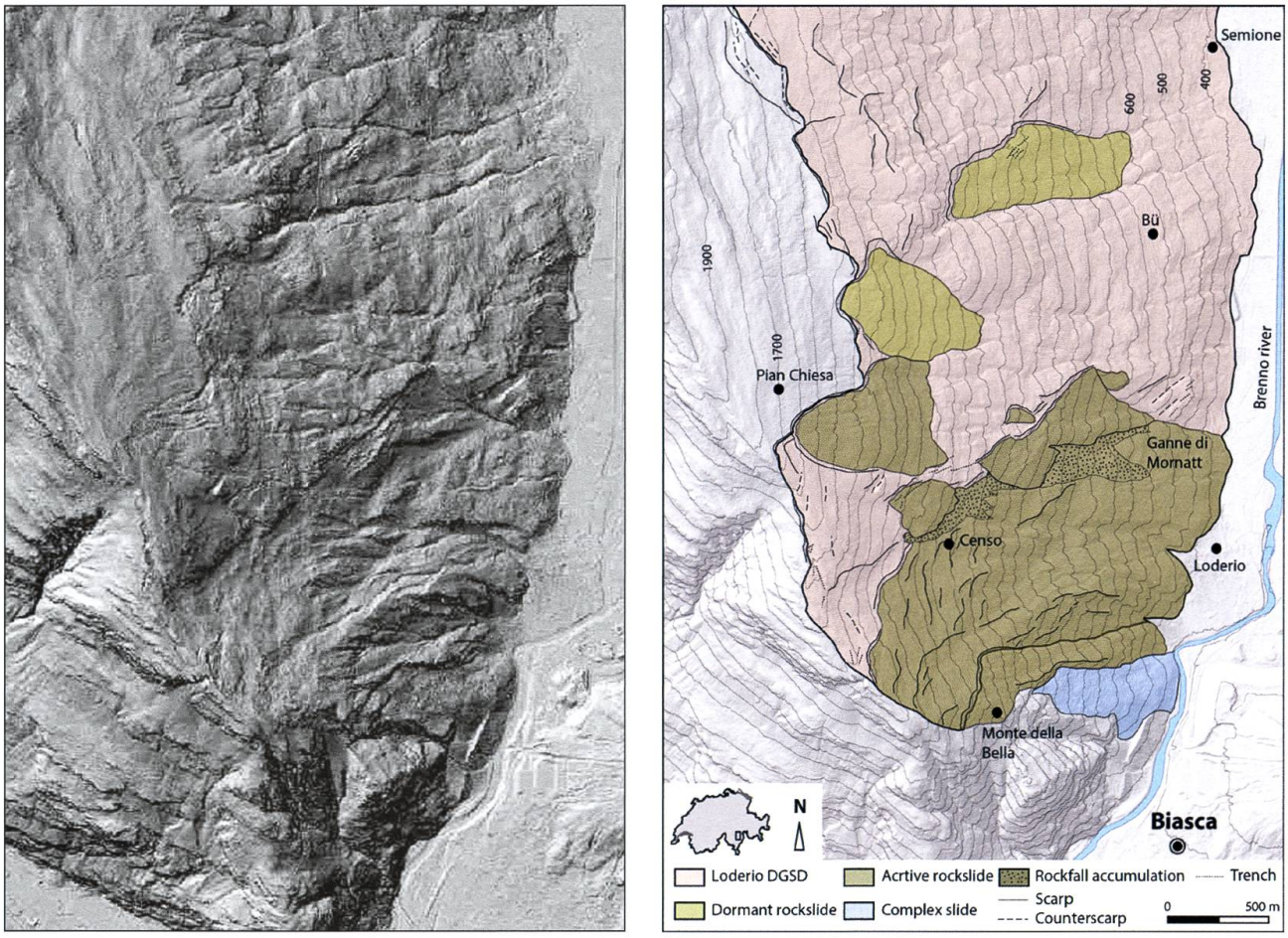

Fig. 2: Shaded relief of a Digital Elevation Model (swissALTI3D copyright 2019 of Swisstopo) and map of the phenomena of the Loderio landslide.

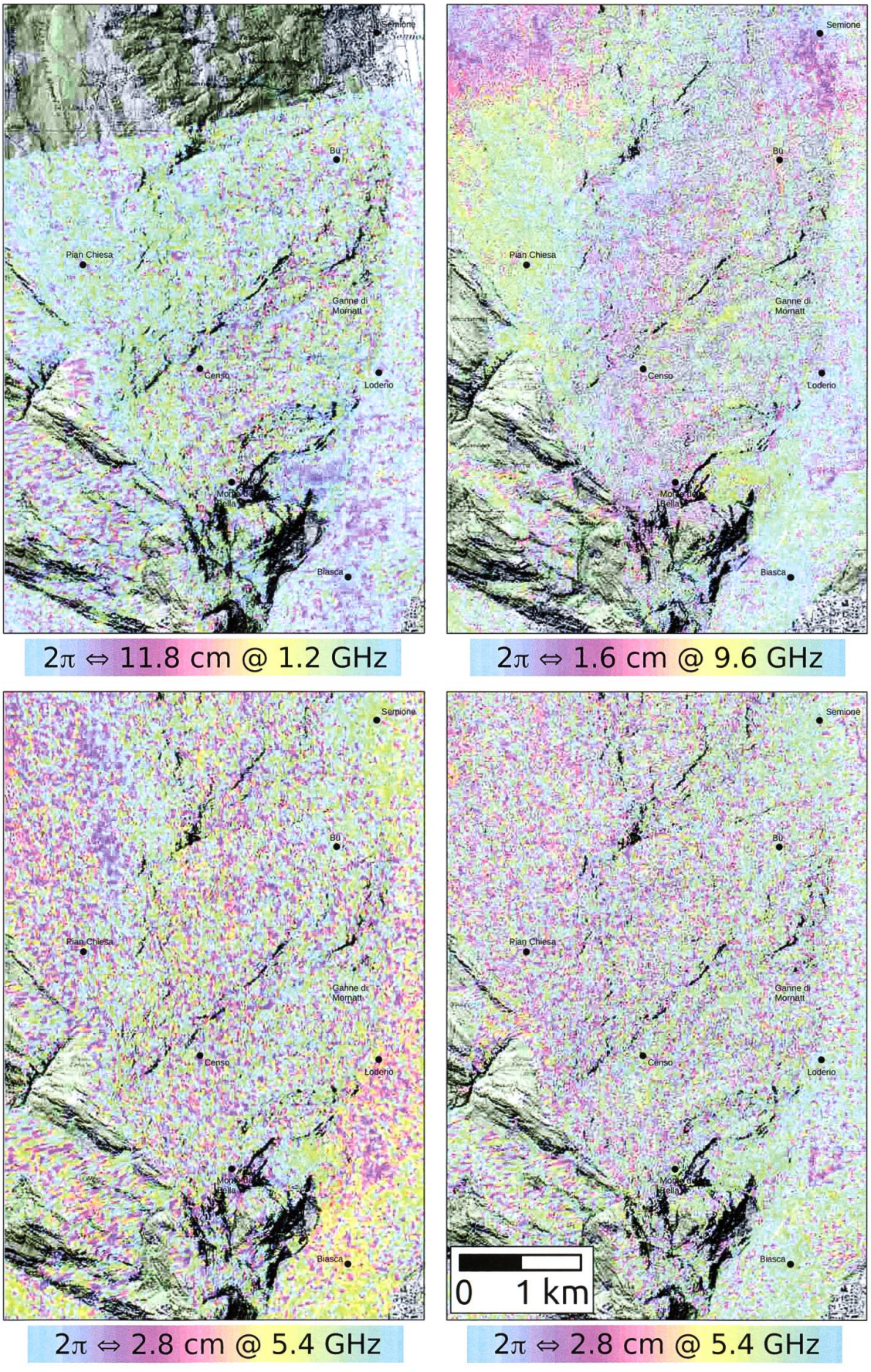

Fig. 3 left to right, top to bottom: DInSAR from ALOS-2 PALSAR-2 between 2017.09.02 and 2017.10.28 (56 days, mean coherence 0.20), TerraSAR-X between 2017.09.23 and 2017.10.04 (11 days, mean coherence 0.15), Sentinel-1 between 2017.09.26 and 2017.10.08 (12 days, mean coherence 0.15) and Radarsat-2 between 2017.09.18 and 2017.10.12 (24 days, mean coherence 0.10). The legend indicates the apparent displacement corresponding to a phase cycle.

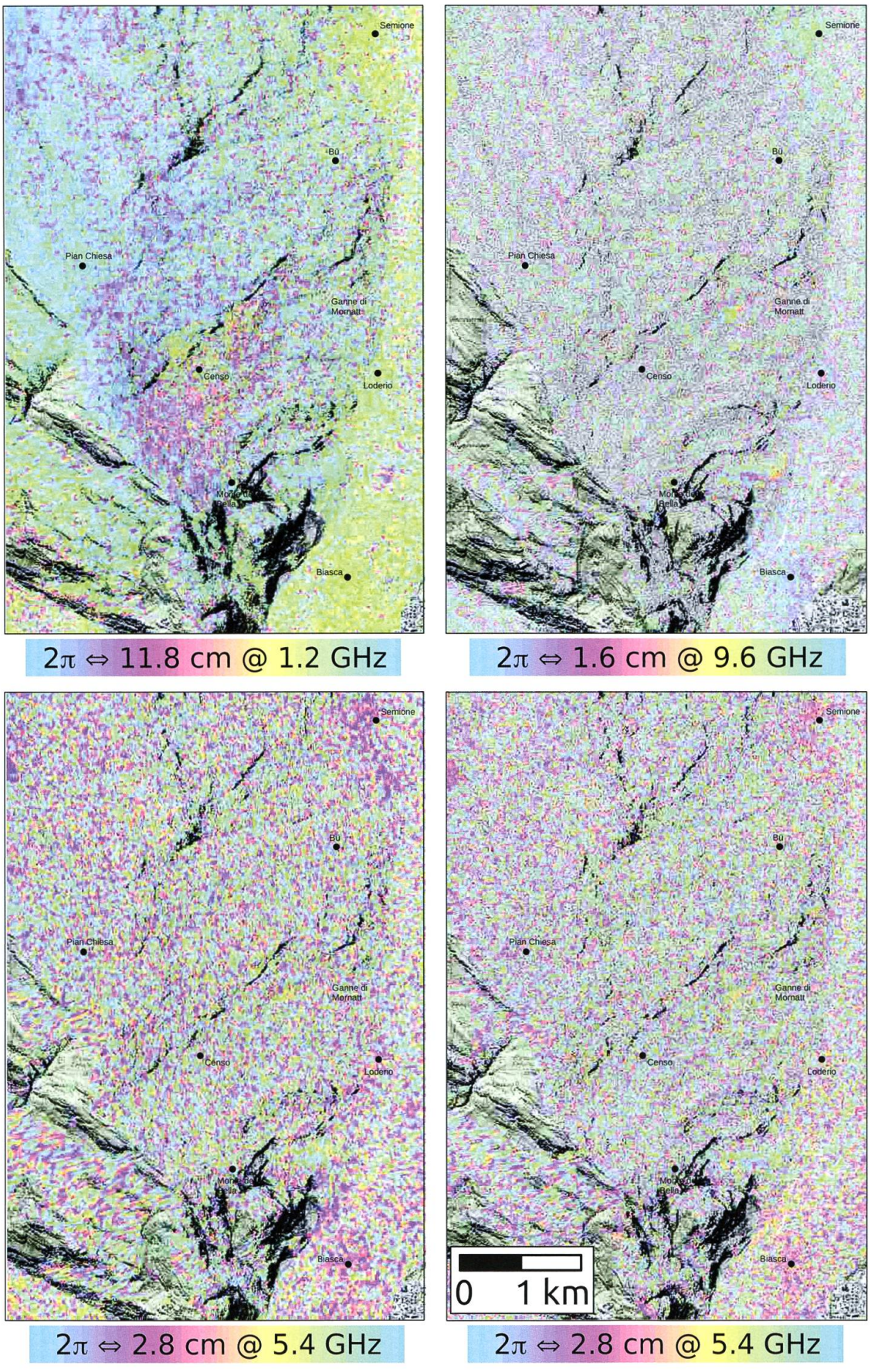

Fig. 4, left to right, top to bottom: DIN SAR from ALOS-2 PALSAR-2 between 2014.09.06 and 2015.09.05 (364 days, mean coherence 0.22), TerraSAR-X between 2016.10.28 and 2017.10.04 (341 days, mean coherence 0.09), Sentinel-1 between 2016.09.25 and 2017.09.26 (366 days, mean coherence 0.11) and Radarsat-2 between 2016.09.23 and 2017.10.12 (384 days, mean coherence 0.10). The legend indicates the apparent displacement corresponding to a phase cycle.

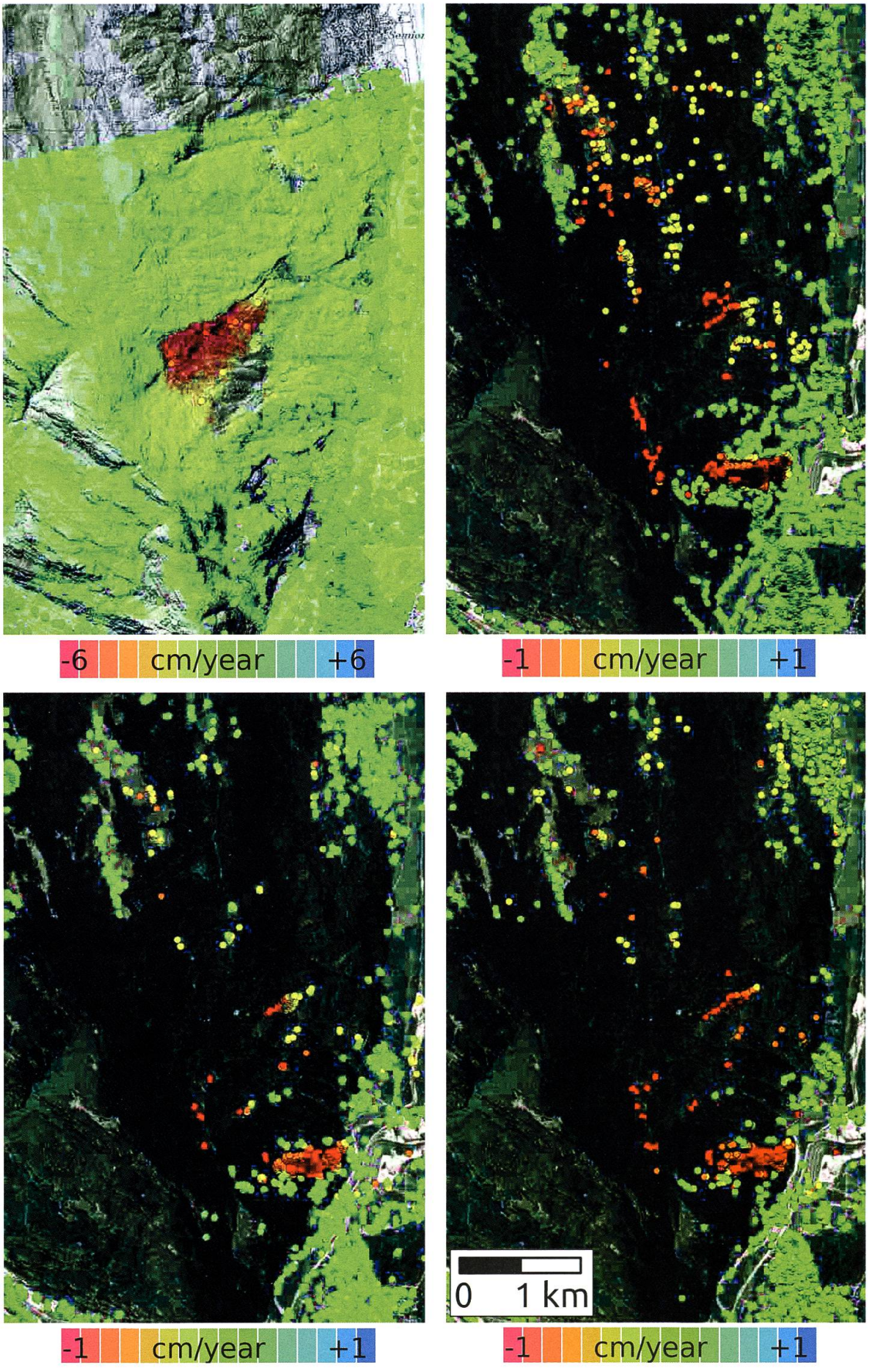

Fig. 5, left to right, top to bottom: MTI LOS displacement mapsfrom ALOS-2 PALSAR-2 between 2014 and 2018 and PSI LOS displacement maps from ALOS-2 PALSAR-2 between 2014 and 2018, TerraSAR-X between 2014 and 2017, SENTINEL-1 between 2015 and 2018 and Radarsat-2 between 2011 and 2017. The colour scale is saturated at 6 cm/year for ALOS-2 PALSAR-2 and at 1 cm/year for the three other sensors.

ley and over the meadows in the north-west, while within the forest good coherence can be only observed over the accumulations of debris by reason of the very good spatial resolution of this sensor. Moreover, at C-band over 12 days (Sentinel-1) the phase signal is only visible at the bottom of the valley and over the meadows in the north-east, while over 24 days only the bottom of the valley is fairly coherent in spite of the better spatial resolution of Radarsat-2 with respect to Sentinel-1. We finally remark that with all the current considered satellite missions the baselines are consistently short and therefore low spatial coherence is no more a limitation of the technology.

Differential interferograms over about one year from ALOS-2 PALSAR-2, TerraSAR-X, Sentinel-1 and Radarsat-2 at the end of the summer / beginning of autumn are presented in Figure 4. With ALOS-2 PALSAR-2 a fairly good coherence can be observed over the whole region of interest. Because at L-band backscattering originates from large branches, trunks and the ground instead of the vegetation canopy (Strozzi et al., 2005), the signal of the fastest moving part of the landslide is visible within the forest. At X- and C-band, on the other hand, we observe small patches of coherence only over the villages at the bottom of the valley and the accumulations of debris, in particular for TerraSAR-X and Radarsat-2 having a better spatial resolution than Sentinel-1. With the higher frequencies, vegetated areas (forest and meadows) are completely decorrelated over one year.

PSI and MTI results consist of linear deformation rates and displacement histories in the satellite LOS direction. We present in Figure 5 the LOS displacement maps from Sentinel-1 and Radarsat-2. Reference points were selected individually for each of the sensors in presumably stable areas. PSI coverage from ALOS-2 PALSAR-2 is sparse and restricted to the lower part of the slope, because the number of acquisitions is limited to 17 and five winter images were included in the analysis. On the other hand, the spatial coverage with valuable information from the MTI analysis of the 12 summer images is much more extended and the deformation rates reach values of up to 6 cm/year in the central forested part of the landslide. With TerraSAR-X, Sentinel-1 and Radarsat-2 PSI rates of motion of a few cm/year are detected over large part of the slope, but not over the fastest moving part of the landslide. The detected points at X- and C-band mainly correspond to buildings and rocks, with clusters of points over settlements and the accumulations of debris. Sentinel-1 and Radarsat-2 PSI analyses are well comparable in terms of the density of points. The PSI analysis from TerraSAR-X greatly increases the point density.

6 Discussion

L-band MTI is complementary to C- and X-band PSI for the study of landslides. L-band is less affected than C- and X-band by temporal decorrelation over vegetated areas and relatively fast movements. For this reason, the fastest moving part of the Loderio landslide could be only detected with ALOS-2 PALSAR-2 data. On the other hand, C- and X-band are more sensitive to the very slow-moving sectors of the landslide, with very-high spatial resolution TerraSAR-X data preferred to increase the point density and studying local phenomena. In spite of the large number of TerraSAR-X, Sentinel-1 and Radarsat-2 acquisitions available, points moving with velocities larger than a few cm/year could not captured with these sensors, because processing has to be limited to summer acquisitions with long time intervals spanning winter months.

The satellite-based interferometric analyses confirm the extension of the Loderio DGSD determined from the morphostructures detected in the field and from photointerpretation. Over the northern sector of the Loderio

DGSD above Semione, which did not appear to be particularly active from geomorphological indicators, the Sentinel-1, Radarsat-2 and TerraSAR-X PSI results indicate indeed limited LOS rates of motion of a few mm/year. The rates of deformation progressively decrease from the upper to the lower part of the slope, as observed by other authors for similar phenomena (Dramis and Sorriso-Valvo, 1994; Noverraz et al., 1998; Raspini et al, 2016; Frattini et al., 2018). The central sector of the Loderio DGSD is slightly more active than the northern sector. In particular, the displacement map from Terra SAR-X confirms that the rockslide in the center of the slope is an active phenomenon with LOS deformation rates on the order of 1 cm/year, in accordance with the field observation.

In the southern sector of the Loderio DGSD LOS movements larger than 1 cm/year can be observed with Sentinel-1, Radarsat-2 and TerraSAR-X PSI on the deposits of debris and on the holiday houses in Censo. However, the active deformation of the upper slope with sliding and tilting of the rockmass, where LOS deformation rates reach values of up to 6 cm/year (or up to 7 cm/year if projected along the slope direction), is only discriminated with the ALOS-2 PALSAR-2 data. In this area, small rock falls are frequently observed. The small rock falls are therefore not the consequence of local instabilities, but part of a continuous and progressive deformation of the slope. The movements in the accumulation of the complex rockslide in the most southern part of the slope can be well observed with all SAR missions with LOS rates of motion larger than 1 cm/year. These movements associated with the active deformation of the scarp show the kinematic of this complex landslide with a combination of rockfalls and slide of the debris accumulation. Information on surface displacement from PSI and MTI can be now combined with the landslide inventory to assign the state of activity of the various sectors of the Loderio landslide (Strozzi et al., 2013; Ambrosi et al., 2018).

7 Summary and outlook

We presented the results over an exemplary slow-moving landslide located in Ticino by considering multiple SAR sensors and discussed potential and limitations of different carrier frequencies, ground resolutions, time intervals and acquisition strategies. With these data, we envisage in the coming years the following general opportunities over Switzerland. Sentinel-1 PSI can provide an operational and efficient tool for a systematic national monitor, thanks to the large number of images regularly acquired every 6 to 12 days since 2014 and distributed with an open policy. ALOS-2 PALSAR-2 are also systematically acquired over the whole country since 2014, but the number of images is limited to a few every year. In addition, data are expensive or distributed with strict restrictions for scientific use. Therefore, ALOS-2 PALSAR-2 can be mainly employed to compute selected differential interferograms, with limited studies feasible with MTI. TerraSAR-X, Radarsat-2 and Cosmo-SkyMed data are acquired since 2008 only over selected regions subject to programming and PSI processing can be performed on demand over these areas for local studies.

In addition to the study of slow-moving landslides, multi-temporal interferometric approaches based on large data stacks offer the possibility to study other types of ground motion, such as subsidence (e.g. over deltas on lakes), settlements over underground constructions (e.g Strozzi et al., 2017) or slow periglacial phenomena (e.g. Delaloye et al., 2007). For the study of slow (i.e. rates of motion of a few m/a according to Cruden and Varnes, 1996) process-scale phenomena, DinSAR data with short time intervals can be employed where coherence is preserved. In particular for the alpine areas, rock glaciers, landslides and other periglacial phenomena can be analysed during summer months and in winter under dry snow conditions (e.g. Strozzi et al., 2010; Barboux et al., 2011; Barboux et al., 2015; Manconi et al., 2018).

In near future promising new perspectives for the monitoring of very slow landslides with satellite SAR interferometry arise from new sensors, initiatives and algorithms. The Copernicus Sentinel-1 satellite constellation will be complemented with two further sensors at C-band (Sentinel-1C and 1D[3]). At L-band, new sensors are under development at JAXA (ALOS-4 PALSAR-3[4]), ESA (ROSE-L[5]) and NASA (NISAR[6]). X-band commercial sensors will be launched not only by public institutions (e.g. the German, Italian and Spanish space agencies), but also private companies (e.g. ICEYE, Capella Space, and Synspective). New national and international initiatives (e.g. the pan-European PSI processing, i.e. the future «European Ground Motion Service» by Copernicus[7]) will open the use of displacement data to non InSAR specialist. Finally, it is expected that continuous improvements in algorithm's development will make InSAR time-series reconstruction more robust and operational.

Acknowledgments

The research leading to these results received funding from the «Programma di cooperazione Interreg V-A Italia-Svizzera 2014-2020» within the projects «Sicurezza delle infrastrutture critiche transfrontaliere (SICT)» and «Alpi in Movimento, movimento nelle Alpi – Piuro 1618 (AMALPI18)», the Swiss Federal Office for the Environment within the project «InSAR Auswertungen 2019», and the European Space Agency (ESA) within the «L-band SAR Applications and Requirements Consolidation Study». ALOS-2 PALSAR-2 data are courtesy of RA6_3016, copyright JAXA. Sentinel-1 images available from Copernicus. TERRASAR-X data are courtesy of GEO3647, copyright DLR. Radarsat-2 data are copyright MDA. SwissAlti3D is copyright 2015 of Swisstopo, Swissimages are copyright 2020 of Swisstopo (BAT200006).

References

Ambrosi, C., Strozzi, T., Scapozza, C. & Wegmüller, U., 2018: Landslide hazard assessment in the Himalayas (Nepal and Bhutan) based on Earth-Observation data. Engineering Geology, 237: 217-228, doi: 10.1016/j.enggeo.2018.02.020.

Bamler, R. & Hartl, P., 1998: Synthetic aperture radar interferometry. Inverse Problems, 14, R1–R54.

Barboux, C., Delaloye, R., Strozzi, T., Collet, C. & Raetzo, H., 2011: TSX InSAR assessment for slope instabilities monitoring in alpine periglacial environment (Western Swiss Alps, Switzerland). Proceedings of the FRINGE 2011 workshop, 19-23 September (ESA SP-697, January 2012).

Barboux, C., Strozzi, T., Delaloye, R., Wegmüller, U. & Collet, C., 2015: Mapping slope movements in Alpine environments using TerraSAR-X interferometric methods. Journal of Photogrammetry and Remote Sensing, 109, 178-192, 2015, doi:10.1016/j.isprsjprs.2015.09.010.

Berardino, P., Fornaro, G., Lanari, R. & Sansosti, E., 2002: A New Algorithm for Surface Deformation Monitoring Based on Small Baseline Differential SAR Interferograms. IEEE Trans. Geosc. Rem. Sens. 40(11).

Caduff, R., Strozzi, T., Wiesmann, A. & Wegmüller, U., 2017: Monitoring glacial, periglacial and landslide surface motion with Sentinel-1 over the Swiss Alps every 6 days, 15th Swiss Geosci-

3 https://www.copernicus.eu/en/sentinel-1c-and-1d-satellites-ordered-esa
4 https://global.jaxa.jp/projects/sat/alos4
5 https://www.esa.int/Our_Activities/Observing_the_Earth/Copernicus/Candidate_missions
6 https://nisar.jpl.nasa.gov
7 https://land.copernicus.eu/user-corner/technical-library/european-ground-motion-service

ence Meeting, Davos, 17-18 November.
Colesanti, C. & Wasowski, J., 2006: Investigating landslides with space-borne Synthetic Aperture Radar (SAR) interferometry. Eng. Geol. 88(3-4), 173-199.
Crosetto, M., Monserrat, O., Bremmer, C., Hanssen, R., Capes, R. & Marsh, S., 2009: Ground motion monitoring using SAR interferometry: quality assessment. Eur. Geol. 26, 12–15.
Cruden, D.M. & Varnes, D.J., 1996: Landslide Types and Processes. In: Turner, A.K. and Shuster, R.L., Eds., Landslides: Investigation and Mitigation, Transportation Research Board, Special Report No. 247: 36-75.
Delacourt, C., Allemand, P., Berthier, E., Raucoules, D., Casson, B., Grandjean, P., Pambrun, C. & Varel, E., 2007: Remote-sensing techniques for analysing landslide kinematics: a review. Bull. Soc. Geol. Fr. 178 (2), 89–100.
Delaloye, R., Lambiel, C., Lugon, R., Raetzo, H. & Strozzi, T., 2007: ERS InSAR for detecting slope movement in a periglacial mountain environment (western Valais Alps, Switzerland). Proceedings HMRSC-IX, Graz, 14-15 Sept. 2006, Grazer Schriften der Geographie und Raumforschung 43, 113-120.
Dramis, F. & Sorriso-Valvo, M., 1994 : Deep-seated gravitational slope deformations, related landslides and tectonics. Engineering Geology, 38(3–4): 231-243.
Ferretti, A., Prati, C. & Rocca, F., 2001: Permanent scatterers in SAR interferometry. IEEE Trans. Geosci. Remote Sens. 39 (1), 8–20.
Frattini, P., Crosta G.B., Rossini M. & Allievi J. 2018: Activity and kinematic behaviour of deep-seated landslides from PS-InSAR displacement rate measurements. Landslides. 15 (6), 1052-1070.
Herrera, G., Davalillo, J.C., Mulas, J., Cooksley, G., Monserrat, O. & Pancioli, V., 2009: Mapping and monitoring geomorphological processes in mountainous areas using PSI data: central Pyreneescase study. Nat. Hazards Earth Syst. Sci. 9, 1587-1598.
Hooper, A., 2008. A multi-temporal InSAR method incorporating both persistent scatterer and small baseline approaches. Geophysical Research Letters. 35(16).
Krähenbühl, R. & Nänni, C., 2017: Ist das Dorf Brienz-Brinzauls Bergsturz gefährdet? Swiss Bulletin for Applied Geology. 22(2).
Lateltin, O., Haemmig, C., Raetzo, H. & Bonnard, C 2005: Landslide risk management in Switzerland. Landslides 2005, 2, 313–320.
Manconi, A., Kourkouli,P., Caduff, R., Strozzi, T. & Loew, S., 2018 : Monitoring Surface Deformation over a Failing Rock Slope with the ESA Sentinels: Insights from Moosfluh Instability, Swiss Alps. Remote Sens., 10(5), 672.
Ng, A.H.-M., Ge, L., Li, X., Abidin, H.Z., Andreas, H. & Zhang, K., 2012: Mapping land subsidence in Jakarta, Indonesia using persistent scatterer interferometry (PSI) technique with ALOS PALSAR. Int. J. Appl. Earth Obs. Geoinf. 18, 232–242.
Nishiguchi, T., Tsuchiya, S. & Imaizumi, F., 2017: Detection and accuracy of landslide movement by InSAR analysis using PALSAR-2 data. Landslides 14, 1483–1490.
Noverraz, F., Bonnard, C., Dupraz, H. & Uguenin, L, 1998: Grands Glissements de Versants et Climat; Nationales Forschungsprogramm «Klimaänderungen und Naturkatastrophen» (NFP 31), Schlussbericht; Hochschulverlag AG an der ETH: Zurich, Switzerland, p. 316.
Palmer J. 2017: Creeping earth could hold secret to deadly landslides, Nature, 548(384-386).
Raetzo, H. & Loup, B., 2016: Protection Against Mass Movement Hazards - Guideline for the Integrated Hazard Management of Landslides, Rockfall and Hillslope Debris Flows. Published by the Federal Office for the Environment FOEN, Bern, Switzerland.
Raspini, F., Bardi, F., Bianchini, S., Ciampalini, A., Del Ventisette, C., Farina, P., Ferrigno, F., Solari, L. & Casagli, N., 2016 : The contribution of satellite SAR-derived displacement measurements in landslide risk management practices. Natural Hazard 86 (1), 327-351.
Rosen, P., Hensley, S., Joughin, I., Li, F., Madsen, S. & Rodriguez, E. 2000: Goldstein, R. Synthetic aperture radar interferometry. Proceedings of the IEEE 2000, 88, 333–382.
Sandwell, D., Myer, D., Mellors, R., Shimada, M., Brooks, B. & Foster, J. 2008: Accuracy and resolution of ALOS interferometry: vector deformation maps of the father's day intrusion at Kilauea. IEEE Trans. Geosci. Remote Sens. 46 (11), 3524–3534.
Samiei-Esfahany, S., Martins, J.E., van Leijen, F. & Hanssen, R.F. 2016: Phase Estimation for Distributed Scatterers in InSAR Stacks Using Integer Least Squares Estimation. IEEE Trans. Geosc. Rem. Sens. 54(10).
Schmidt, D. & Bürgmann, R., 2003: Time-dependent land uplift and subsidencein the Santa Clara valley, California, from a large interferometric synthetic aperture radardata set. Journal of Geoph. Res. 108(B9), 2416.
Strozzi T., Farina, P., Corsini, A., Ambrosi, C., Thüring, M., Zilger, J., Wiesmann, A., Wegmüller, U. & Werner, C. 2005: Survey and monitoring of landslide displacements by means of L-band satellite SAR interferometry. Landslides, Vol. 2, No. 3, pp. 193 – 201, doi: 10.1007/s10346-005-0003-2, 2005.
Strozzi, T., Delaloye, R., Kääb, A., Ambrosi, C., Perruchoud, E. & Wegmüller, U. 2010: Combined observations of rock mass movements using satellite SAR inteferometry, differential GPS, airborne digital photogrammetry, and airborne photography interpretation. J. Geophys. Res. 2010, 115, F01014.
Strozzi, T., Ambrosi, C., & Raetzo, H. 2013: Interpretation of Aerial Photographs and Satellite SAR Interferometry for the Inventory of Landslides, Remote Sensing, 5(5): 2554-2570.
Strozzi, T., Caduff, R., Wegmüller, U., Raetzo, H. &

Hauser, M., 2017: Widespread surface subsidence measured with satellite SAR interferometry in the Swiss alpine range associated with the construction of the Gotthard Base Tunnel. Remote Sensing of Environment, 190: 1-12, doi: 10.1016/j.rse.2016.12.007.

Wasowski, J. & Bovenga, F., 2014: Investigating landslides and unstable slopes with satellite Multi Temporal Interferometry: Current issues and future perspectives. Engineering Geology, 174: 103-138, doi: j.enggeo.2014.03.003.

Wegmüller, U., Werner, C., Strozzi, T. & Wiesmann, A., 2003: Multi-temporal interferometric point target analysis. In: Proceedings of Multi-Temp 2003 Conference, Ispra, Italy.

Wegmüller, U., Strozzi, T., & Gruner, U. 2013: Verschiebungsmessungen mittels Satellitenradar im Urner Reusstal oberhalb der Nord-Süd-Verkehrsachse im Zeitraum 1992 – 2010, Swiss Bull. angew. Geol., 18(2): 139-153.

Werner, C., Wegmüller, U. & Strozzi, T., 2012: Deformation time-series of the Lost-Hills oil field using a multi-baseline interferometric SAR inversion algorithm with finite difference